Original Research Article

Lignin precursors enhance exolaccase-started humification of bisphenol A to form functional polymers

Shunyao Li [a], Dan Hong [b], Kai Sun [b,c,*]

[a] *Laboratory of Wetland Protection and Ecological Restoration, Anhui University, Hefei 230601, China*
[b] *Anhui Province Key Laboratory of Farmland Ecological Conservation and Pollution Prevention, College of Resources and Environment, Anhui Agricultural University, Hefei 230036, China*
[c] *CAS Key Laboratory of Urban Pollutant Conversion, Department of Environmental Science and Engineering, University of Science and Technology of China, Hefei 230026, China*

ARTICLE INFO

ABSTRACT

Humification plays a significant role in converting phenolic pollutants and forming heterogeneous polymers, but few studies have been performed to investigate exolaccase-started humification (ESH). Herein, the influences of lignin precursors (LPs) on exolaccase-induced bisphenol A (BPA) removal and humification were explored. In particular, the architectural features and botanical effects of the formed humification products were also tested. ESH was extremely beneficial in boosting BPA removal in the presence of LPs. Compared with LP-free (58.49%), 100% of BPA was eliminated after the reaction with ESH for 72 h. Such a process was controlled by an exolaccase-caused random assembly of radicals, which generated a large number of hydrophobic polymers through nonspecific covalent binding of C–C and/or C–O. These humified polymers were extremely stable at pH 2.0–10.0 and −20 °C to 80 °C and displayed unique functions, *i.e.*, scavenged 2,2-diphenyl-1-picrylhydrazyl/2,2′-azino-bis3-ethylbenzothiazoline-6-sulphonic acid radicals and exerted antioxidant capacities. More importantly, the functional polymers could act as auxin analogs to increase the germination index (>100%), plant biomass, and salt tolerance of radish seedlings. Our findings disclosed that ESH could not only be optimized to mitigate the ecological risks of phenolic pollutants and sequester organic carbon in environmental bioremediation, but the resulting abundant auxin analogs also contributed to agricultural productivity.

1. Introduction

In global biogeochemical cycles, the conversion of phenolic pollutants involves two opposing modes, *i.e.*, decomposition and humification [1,2]. Decomposition can destroy the chemical structure of contaminants to generate smaller and more labile species [3,4]. Inversely, humification is a process in which phenolic pollutants are incorporated into stable and harmless polymers [5,6]. Both conversion pathways favor avoiding the risk of organic contamination [2,7]. In recent years, humification process has attracted great attention in bioremediation, owing to its capability to regulate phenolic pollutants, stabilize organic matter, and reduce CO_2 emissions [8]. The co-polymerization of phenolic contaminants and small precursors is one of the classic research topics in the field of humification, which can be dominated by certain metal oxides and oxidative enzymes [9, 10]. Such a humification model has high potential in decontamination of phenolic pollutants, and contributes to creating functional polymers [11–13].

Lignin precursors (LPs), such as catechol (Cat), vanillic acid (Vaa), gallic acid (Gaa), and ferulic acid (Fea), are universally found in water ecosystems [14,15]. They have long been regarded as a low-cost feedstock for the production of functional polymers during humification [16–18]. In the complicated humification process, the hazards of phenolic pollutants can be annihilated in the presence of LPs [8]. It is probably because LPs, organic contaminants, aromatic components, and other compounds undergo a series of oxidative coupling reactions to produce advanced humic molecules [19,20]. One key issue is that natural humification is greatly lengthy without sufficient catalysts [21]. Fortunately, the humification process can be significantly facilitated by the artificial addition of appropriate reaction catalysts, such as certain metal oxides (*i.e.*, MnO_2, Al_2O_3, and Fe_2O_3) and oxidative enzymes (*i.e.*, laccase, tyrosinase, and peroxidase) [19].

As described above, the presence of metal catalysts is essential for enhancing the removal and humification of phenolic pollutants [21,22]. By obtaining electrons from substrates, certain metal oxides can act as

---

* Corresponding author.
   E-mail address: sunkai@ahau.edu.cn (K. Sun).

Lewis acids to stimulate nucleophilic addition and polycondensation [23, 24]. Compared with metal oxides, the unique arrangement of reactive centers in enzymes contributes to demonstrating their stronger humification potential [19]. Exolaccase, as a "green and almighty catalyst", can propel the humification of multitudinous phenolic pollutants in the absence of H_2O_2 [8,20]. The substrates are commonly converted into phenoxy radical intermediates by exolaccase, which can be randomly polymerized to generate macromolecular precipitates [25]. The reaction kinetics of phenolic pollutants mediated by exolaccase-started humification (ESH) has been reported [26–28], but little information is available on the role of LPs in eliminating phenolic pollutants and forming functional polymers.

In our study, bisphenol A (BPA, an organic pollutant with estrogenic activity) was selected as a typical phenolic contaminant to explore the effects of LPs on BPA removal and humification caused by ESH. The kinetic model of BPA removal was investigated in ESH by batch experiments. The micromorphologies, functional groups, and chemical structures of the formed humification products were analyzed through scanning electron microscopy (SEM), Fourier transform infrared spectroscopy (FTIR), and ^{1}H nuclear magnetic resonance (^{1}H NMR). Environmental stabilities and radical scavenging activities of humified products were carefully measured. Subsequently, the botanical effects of humified products were also assessed by greenhouse pot experiments. These findings provided a better understanding of the influence of ESH on the co-polymerization and humification of phenolic contaminants and LPs, which was beneficial to circumventing the environmental risks of organic pollutants, sequestering organic carbon, and acquiring functional polymers.

2. Materials and methods

2.1. Chemicals and materials

Four representative LPs (*i.e.*, Cat, Vaa, Gaa, and Fea), BPA, 2,6-dimethoxyphenol (2,6-DMP), and *Trametes versicolor* exolaccase were purchased from Sigma-Aldrich (St. Louis, MO, USA). High-performance liquid chromatography (HPLC)-grade methanol and acetonitrile were obtained from Fisher Scientific (Pittsburgh, PA, USA). All other chemicals were analytical-grade chemicals from Aladdin Industrial Corporation (Shanghai, China). ESH was established in a 10 mM citrate-phosphate buffer solution (C-PBS). Radish (*Raphanus sativus* L.) seeds from Anhui Academy of Agriculture Sciences (Hefei, China) were pre-germinated in a sterile Murashige & Skoog (MS) medium (MDBio, Inc., Taiwan, China) containing 0.6% agar (w/v).

2.2. Batch experiments

To investigate the effects of a mixture of different LPs on BPA removal kinetics, ESH was carried out in a 10 mM C-PBS. Five treatment groups were set in the experiments: (1) exolaccase + BPA (La–BPA); (2) exolaccase + BPA + Cat + Vaa (La–BPA–Cat–Vaa); (3) exolaccase + BPA + Cat + Gaa (La–BPA–Cat–Gaa); (4) exolaccase + BPA + Cat + Fea (La–BPA–Cat–Fea); (5) exolaccase + BPA + Cat + Vaa + Gaa + Fea (La–BPA–Cat–Vaa–Gaa–Fea). Another main purpose was to produce structurally complex humification products. Each reactor initially contained 500 mL of 10 mM C-PBS. Concentrated stock solutions of BPA and LPs were sequentially injected into the reactor to obtain 0.1 mM BPA and 1.0 mM LP (BPA:LP = 1:10, molar ratio; the content of each LP was 1.0 mM in different treatment groups). The enzymatic reaction was immediately initiated by adding 1.0 U/mL exolaccase. The reaction was set to proceed for 72 h at 25 °C, pH 5.0, and 150 r/min. The solution pH was set to 5.0, as it was the optimal pH for exolaccase-induced removal of phenolic contaminants. At the selected time interval, a 1 mL sample was promptly taken and then quenched with an equal volume of methanol to measure BPA concentration. Exolaccase activity was routinely assayed at 468 nm using 2,6-DMP as a chromogenic substrate [29]. All experiments were conducted in triplicate.

2.3. High-performance liquid chromatography (HPLC) and high-resolution mass spectrometry (HRMS) analysis

A Waters HPLC system (Milford, MA, USA) equipped with an Agilent ZORBAX Eclipse Plus C18 column (4.6 mm × 150 mm, 5 μm particle size) was employed for BPA determination. The mobile phase consisted of an acetonitrile component (A) and an aqueous component (B). BPA concentration was analyzed with a 1.0 mL/min flow of mobile phase consisting of 70% A and 30% B by an ultraviolet detector at 278 nm. Each reaction corresponding to BPA concentration was monitored in triplicate. The treatment groups without exolaccase were also conducted, and no evidence of BPA removal was observed. BPA concentration was quantifically detected by the multipoint standard calibration curves. The humified products of BPA were recognized by LTQ-Orbitrap HRMS (Thermo Fisher Scientific, Bremen, Germany). ESH was terminated for a 6 h incubation by acidifying to pH 2.0. Then, the samples were concentrated, dried, and re-dissolved in HPLC-grade methanol for HRMS identification. The detailed operation conditions of HRMS were given in the Supplementary Information (SI).

2.4. Performance measurement of humified products

In our study, four humified precipitates (*i.e.*, La–P1, La–P2, La–P3, and La–P4) were collected from La–BPA–Cat–Vaa, La–BPA–Cat–Gaa, La–BPA–Cat–Fea, and La–BPA–Cat–Vaa–Gaa–Fea, respectively. After a 3 d humification, the reaction solutions were adjusted to pH 2.0. Subsequently, the humified products were fully precipitated by standing for 24 h. The resulting precipitates were centrifugally separated, washed with deionized water 3 times, and freeze-dried. The particle sizes and morphologies of humified precipitates were determined using SEM (HITACHI S-4800, Japan; voltage of 5 kV, 10,000 times). FTIR spectra (NEXUS870, NICOLET, USA) of humified precipitates were determined in the range of 400–4,000 cm^{-1} (scanning interval of 2 cm^{-1}, an average of 64 scans). The humified precipitates (5 mg) were dissolved in dimethylsulfoxide-d_6 (DMSO-d_6) reagent, and ^{1}H NMR (Agilent Technologies, USA) was used to record the chemical structures of samples. BPA–Cat–Vaa (Hm–P1), BPA–Cat–Gaa (Hm–P2), BPA–Cat–Fea (Hm–P3), and BPA–Cat–Vaa–Gaa–Fea (Hm–P4) monomer mixtures (molar ratio = 1:10) were also prepared for comparison.

2.5. Environmental stabilities of humified products

The effects of pH (2.0–10.0), temperature (−20 °C to 80 °C, pH 7.0), ultrasonic duration (1–5 h, with a frequency of 50 Hz, pH 7.0), and exposure time (5–30 d, pH 7.0) on the environmental stabilities of four humified precipitates were evaluated by the stationary culture with a 14 h white light/10 h darkness cycle at 25 °C. The release amount of BPA monomer is calculated by the following equation:

$$\text{Mass percentage } (\%) = M_{BPA-t} \div M_{BPA-0} \times 100\% \tag{1}$$

where M_{BPA-t} is the content of BPA released from BPA–LP humified precipitates after E-PH, and M_{BPA-0} is the content of BPA in BPA–LP mixed monomers prior to ESH.

2.6. Radical scavenging activities of humified products

As investigators have previously reported, the radical scavenging activities of four humified products were tested using 2,2-diphenyl-1-picrylhydrazyl (DPPH) and 2,2′-azino-bis3-ethylbenzothiazoline-6-sulphonic acid (ABTS), respectively [30]. For DPPH, after 0.1 mM DPPH was dissolved into ethanol, the humified products (*i.e.*, La–P1, La–P2, La–P3, and La–P4) were added to obtain an initial concentration of 0–16 mg/L. The mixtures were incubated for 30 min at 25 °C, and the absorbance was measured at 517 nm. For ABTS, the formation of ABTS cation radical (ABTS$^+$) was accomplished in the dark at 25 °C for 12 h by combining

7.0 mM ABTS and 2.45 mM potassium persulfate in water. After the ABTS$^+$ solution was diluted with ethanol (absorbance value = 0.7 ± 0.02), the humified products (0–12 mg/L) were added into the mixed solutions to incubate for 30 min at the dark conditions. The absorbance value at 734 nm was evaluated. DPPH/ABTS radical scavenging rate (%) was calculated as follows:

$$DPPH/ABTS \text{ radical scavenging rate } (\%) = [1 - (A - A_i) \div A_0] \times 100\% \tag{2}$$

where A_0, A_i, and A are the absorbances of 2 mL ethanol + 2 mL DPPH/ABTS$^+$, 2 mL ethanol + 2 mL sample, and 2 mL sample + 2 mL DPPH/ABTS$^+$, respectively. The percentage of remaining DPPH/ABTS$^+$ against the sample/standard concentration was plotted to acquire the amount of antioxidant (mM) necessary to decrease the initial concentration of DPPH/ABTS$^+$ by 50% (IC$_{50}$).

2.7. Seed germination test

Radish was selected as the tested plant to explore the effects of four humified products on seed germination and seedling growth. After radish seeds were surface-sterilized and pre-germinated as described earlier [17], 15 seeds were transferred onto semi-solid MS media (0.6% agar) containing La–P1, La–P2, La–P3, and La–P4 (50–200 mg/L), respectively. These seeds were cultivated in a plant growth chamber (HBRG-500LED, Changzhou, China) with a 16 h light period at 25 °C for 4 d, and the seed germination and root length were recorded to calculate germination index (GI) (SI). For comparison, the treatment groups without humified products (blank control, BC) and with BPA–LP monomer mixtures were also conducted.

2.8. Salt tolerance evaluation

Retention of chlorophyll content in the leaves under salt stress has been widely used as an index for NaCl tolerance [31]. As we described earlier, the salt tolerance of radish seedlings was assessed by determining the levels of chlorophyll a, b, and a + b [17]. Briefly, radish seedlings grown for 3 d on solid MS medium were transferred to a fresh medium containing 250 mM NaCl and humified precipitates. After a 7 d cultivation, the leaf tissues were collected and ground to extract chlorophyll. The extracted chlorophyll (supernatant) was analyzed using an ultraviolet and visible spectrophotometer (UV-2550, Shimadzu, Japan). The detailed experimental procedures were shown in SI.

3. Results and discussions

3.1. Removal kinetics of BPA in ESH enhanced by LPs

Natural water bodies receive large amounts of LPs, which play a crucial role in the migration and transformation of phenolic pollutants [32,33]. Exolaccase can induce polymerization of various substrates, thus altering the environmental fate of phenolic contaminants [34]. As described in Fig. S1, the chromatographic peak of BPA (3.25 min) in ESH was matched with the standard, as analyzed by HPLC. Compared with the initial phase of ESH (0 h), the chromatographic peak of BPA disappeared in the presence of LPs after a 72 h humification. Furthermore, the chromatographic peaks of LPs between 2.0 and 3.0 min were significantly reduced and even eliminated, owing to the formation of humified products (broad chromatographic peaks at 1.5–2.0 min). Such results were also in good agreement with other reports on BPA removal using exolaccase [35,36].

To further explore the effects of LPs on exolaccase-induced BPA removal, the transformation kinetics of BPA was evaluated. As illustrated in Fig. 1a, as humification time increased, the color of the solution changed from undertint to typical and charming dark brown. In the absence of LPs, BPA removal by ESH was sluggish and only 58.49%
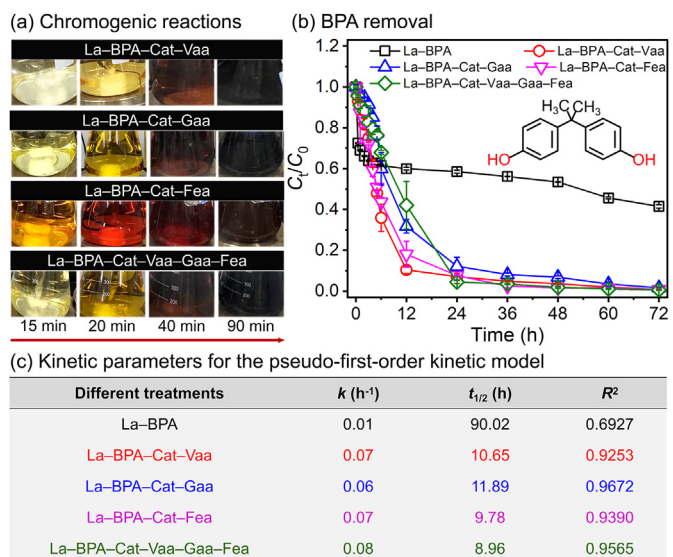
Fig. 1. The presence of LPs enhanced exolaccase-induced BPA removal. (a) Chromogenic reactions; (b) BPA removal; (c) Kinetic parameters for the pseudo-first-order kinetic model. BPA, bisphenol A; LPs, lignin precursors; Cat, catechol; Vaa, vanillic acid; Gaa, gallic acid; Fea, ferulic acid; La–BPA, exolaccase + BPA; La–BPA–Cat–Vaa, exolaccase + BPA + Cat + Vaa; La–BPA–Cat–Gaa, exolaccase + BPA + Cat + Gaa; La–BPA–Cat–Fea, exolaccase + BPA + Cat + Fea; La–BPA–Cat–Vaa–Gaa–Fea, exolaccase + BPA + Cat + Vaa + Gaa + Fea; C_t, the residual concentration of BPA in water at a specific time t; C_0, the initial concentration of BPA in water; k, kinetic constant; $t_{1/2}$, half-life.

within 72 h, while BPA removal rapidly increased to 100% in the presence of LPs (Fig. 1b). This enhancement mechanism might be attributed to the co-polymerization of BPA and LPs, thus maintaining exolaccase activity and stability [36,37]. A study by Nguyen et al. [38] also indicated that humic acid could accelerate exolaccase-catalyzed BPA removal by radical coupling. In La–BPA, La–BPA–Cat–Vaa, La–BPA–Cat–Gaa, La–BPA–Cat–Fea, and La–BPA–Cat–Vaa–Gaa–Fea systems, the pseudo-first-order kinetic constants (k, h^{-1}) of BPA transformation were 0.0077, 0.0651, 0.0583, 0.0709, and 0.0774 h^{-1}, respectively; the half-lives ($t_{1/2}$, h) were 90.02, 10.65, 11.89, 9.78, and 8.96 h, respectively (Fig. 1c). Notably, exolaccase-induced BPA removal deviated from the regression model in the absence of LPs ($R^2 = 0.6927$). It is largely because the formed long-chain BPA oligomers significantly reduced enzyme activity and thus inhibited enzymatic reactions. These results suggested that LPs were greatly beneficial to promoting BPA removal and humification during ESH.

3.2. Morphologic, functional, and structural properties of humified precipitates

Based on different raw materials, ESH can produce a series of polymeric precipitates with different morphologies and particle sizes. As shown in Fig. 2, the formed La–P1, La–P2, La–P3, and La–P4 in ESH presented dark brown, dark gray, brownness, and dark brown, respectively. The microscopic morphologies of four humified precipitates were observed using SEM (also listed in Fig. 2). The results indicated that all precipitates had rough surfaces, heterogeneous natures, and very different morphological characteristics. After ESH for 3 d, the yields of four humified precipitates were 54.74%, 30.85%, 87.30%, and 59.29%, respectively. The difference in yields mainly depended on whether the raw materials were easily polymerized into macromolecular precipitates during ESH.

The functional groups potentially involved in four humified precipitates were determined. FTIR spectra revealed a large and wide absorption peak in La–P1, La–P2, La–P3, and La–P4 at around 3,400 cm^{-1}, ascribed to the –OH stretching of phenolic and carboxylic groups (Fig. S2
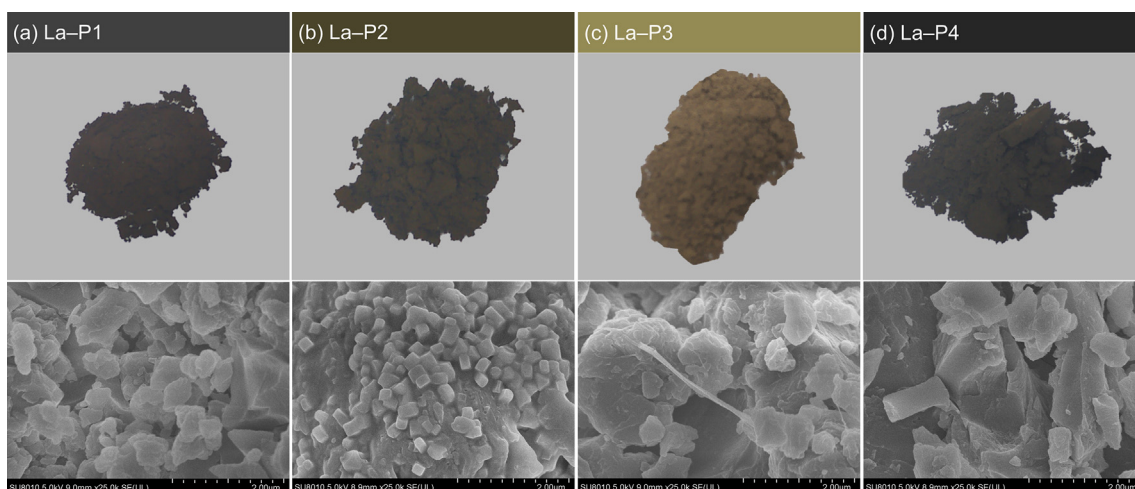
Fig. 2. SEM images of four humified precipitates (*i.e.*, La–P1, La–P2, La–P3, and La–P4). SEM, scanning electron microscopy; La–P1, La–P2, La–P3, and La–P4, four humified precipitates collected from La–BPA–Cat–Vaa, La–BPA–Cat–Gaa, La–BPA–Cat–Fea, and La–BPA–Cat–Vaa–Gaa–Fea, respectively.

and Table S1). The peak between 1,600 and 1,700 cm^{-1} had a sharp band, attributed to the aromatic C=C and conjugated carbonyl C=O stretching [39]. There is a peak position in the region 1,490–1,570 cm^{-1} ascribed to the stretching of carboxyl C–O and C–OH band structures. The peaks from 1,000 cm^{-1} to 1,200 cm^{-1} could be ascribed to the C–O stretching of carboxylic acids, phenols, and aromatic ethers [40].

The ^{1}H NMR spectra of four humified precipitates are described in Fig. S3. The ^{1}H NMR spectra of Hm–P1, Hm–P2, Hm–P3, and Hm–P4 disclosed the representative spectra of BPA-LP monomer mixtures with effective separation between individual NMR resonances. Compared with BPA-LP monomer mixtures, the chemical shift peaks of four humified precipitates in the 3.0–4.0 ppm region were weaker and broader, indicating that the humified products were composed of various oligomers and polymers [39,41]. This is probably because they were randomly polymerized by exolaccase-triggered humification of BPA and LPs [20]. A similar pattern was also observed in the chemical shift region of 6.5–7.5 ppm, where the peaks were almost eliminated in four humified precipitates, manifesting that the dehydrogenation of humified precipitates occurred on the phenolic hydroxyl groups and aromatic rings by radical-caused C–C and/or C–O binding [42]. The differences in peak distribution of the four precipitates appeared because of their different molecular weight and structural characteristics.

3.3. Polymerization mechanisms of BPA and LPs by ESH

The oligomeric products of BPA were tentatively identified using HRMS (Table S2), and the possible humification pathways were proposed in Fig. 3. The predominant pathway of ESH was polymerization, aligning with the result in our previous study [20,36]. According to the humification mechanisms, the polymerization of BPA and LPs could occur through three pathways. First, BPA and LPs were rapidly oxidized at the T1-Cu site (a mononuclear center) to form unstable phenoxyl radical intermediates during ESH [43], as listed in Eqs. 3 and 4. This step has been well-documented by researchers [44,45]. Meanwhile, the dissolved O$_2$ was reduced into H$_2$O at T2/T3-Cu sites (a trinuclear cluster), which had been indirectly confirmed in our study. Because exolaccase-induced BPA removal was completely limited in the absence of O$_2$. Subsequently, these radical intermediates were stochastically coupled to produce the polymeric products [46]. Such a process involved two aspects: one was self-polymerization and the other was co-polymerization [47]. As exhibited in Eqs. 5 and 6, the formed BPA• and LP• were self-coupled to generate self-dimers, self-trimers, self-oligomers, and self-polymers by undergoing continuous C–C and/or C–O binding [19]. These products were still considered to be harmful to the ecosystem and human health
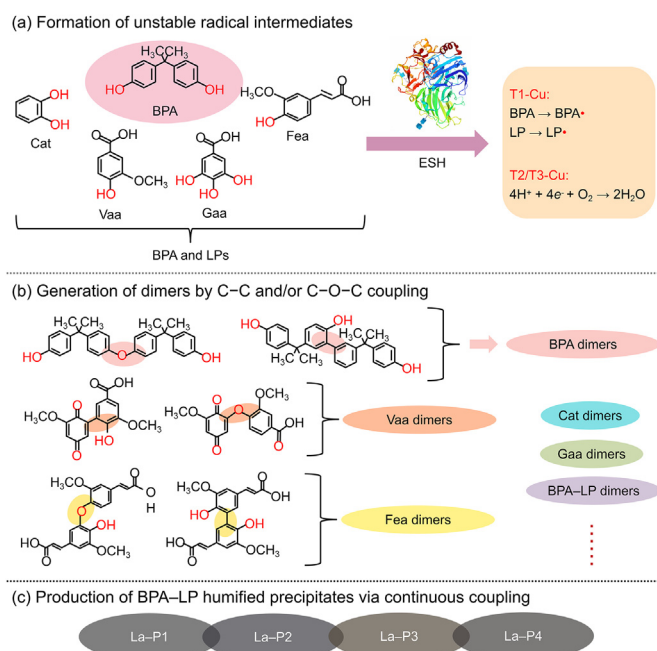
Fig. 3. Proposed pathways for the formation of humified products in ESH. (a) Formation of unstable radical intermediates; (b) Generation of dimers by C–C and C–O coupling; (c) Production of BPA–LP humified precipitates via continuous coupling. ESH, exolaccase-started humification.

[48]. Fortunately, BPA, LP, and their self-polymeric product radicals could encounter co-polymerization via random and uncontrolled reactions to create extremely complicated macromolecular precipitates (Eq. 7), which would be beneficial to avoiding the biotoxicity of BPA–LP monomers and self-polymers [36].

$$4BPA + O_2 \rightarrow 4BPA \cdot + 2H_2O \tag{3}$$

$$4LP + O_2 \rightarrow 4LP \cdot + 2H_2O \tag{4}$$

$$BPA \cdot \rightarrow BPA\ dimers \rightarrow BPA\ trimers \rightarrow \cdots\cdots \rightarrow BPA\ polymers \tag{5}$$

$$LP \cdot \rightarrow LP\ dimers \rightarrow LP\ trimers \rightarrow \cdots\cdots \rightarrow LP\ polymers \tag{6}$$

$$(BPA)_m \cdot + (LP)_n \cdot \rightarrow (BPA)_m - (LP)_n\ copolymers \tag{7}$$
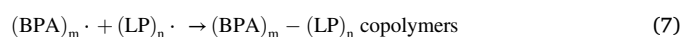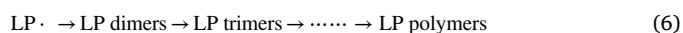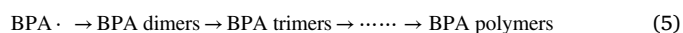
where m and n represent the numbers of BPA and LP monomers, respectively.

3.4. Environmental stabilities of four humified precipitates

As described above, the humified products of BPA and LPs induced by ESH could not only eliminate phenolic contamination but also sequester organic carbon via forming precipitates. However, it is not clear whether the covalent bonds of the formed precipitates would be stable under different environmental conditions. To assess the potential ecological risks of four humified precipitates, the effects of pH, temperature, ultrasonic duration, and exposure time on the re-release of BPA from copolymers were revealed in a light/dark cycle. The release amount of BPA monomer from La–P1, La–P2, La–P3, and La–P4 was 0.11%–1.40% at pH 2.0–10.0, and the maximum BPA release of four copolymers was merely 0.66%, 0.32%, 1.40%, and 0.53%, respectively (Fig. S4a). Similarly, the BPA release of four copolymers was 0.13%–0.88% under different temperatures (Fig. S4b). These results indicated pH and temperature had a negligible effect on the stabilities of C–C and/or C–O covalent bonds.

Considering that ultrasound may destroy the molecular structures of humified precipitates, ultrasonication was also used to treat the four copolymers [49]. With the increase of ultrasonic duration, the BPA release of La–P1, La–P2, La–P3, and La–P4 gradually increased, reaching the maximum values of 0.64%, 0.29%, 1.05%, and 0.26% after 5 h ultrasound, respectively (Fig. S4c). Additionally, the covalent bonds of four copolymers might also be broken by long-term biogeochemical processes [50]. As indicated in Fig. S4d, the release amount of BPA from La–P1, La–P2, La–P3, and La–P4 demonstrated a slight uptrend with the extension of exposure time. Compared with the 5th day, the increment of BPA release on the 30th day was 0.16%, 0.09%, 0.01%, and 0.02%, respectively. The maximum BPA release of four copolymers was less than 1.00%. These results suggested that only a tiny amount of loosely bound BPA was released from BPA–LP copolymers, thus the C–C and/or C–O covalent bonds in four humified precipitates could exist stably in water ecosystems.

3.5. Antioxidant capacities of four humified precipitates

Antioxidants play an essential role in plant defense systems, as they can scavenge reactive oxygen species (ROS) and protect chloroplasts [51, 52]. DPPH/ABTS radical scavenging abilities of four humified precipitates were exhibited in Fig. 4 by antioxidant tests *in vitro*. La–P1, La–P2, La–P3, and La–P4 could scavenge DPPH/ABTS radicals, and the

scavenging rates of DPPH/ABTS radicals were positively correlated with their concentrations ($R^2 > 0.95$). For DPPH, the radical scavenging abilities in four humified precipitates were La–P2 > La–P1 > La–P4 > La–P3. For ABTS, in the presence of 1.0 mg/L La–P1, La–P2, La–P3, and La–P4, the radical scavenging rates of four humified precipitates were 31.78%, 93.51%, 15.89%, and 28.36%, respectively. Subsequently, the IC_{50} values of DPPH/ABTS radicals were calculated by a linear regression model. The IC_{50} was negatively correlated with antioxidant capacity. For instance, the IC_{50} values of DPPH in La–P1, La–P2, La–P3, and La–P4 were 8.36, 1.78, 13.82, and 9.80 mg/L, respectively. The ABTS radical scavenging abilities of four humified precipitates were stronger compared with those of DPPH. It follows that these humified precipitates could effectively scavenge ROS and exert antioxidant capacities, which would help alleviate the biotic and abiotic environmental stimulus at the root surfaces of plants. However, one unsolved issue is whether the precipitates attacked by ROS can produce highly toxic by-products.

3.6. Humified precipitates promoted seed germination

In phytotoxicity tests, certain BPA–LP copolymeric products from ESH could act as auxin analogs to promote seed germination and root length. As shown in Fig. S5, the apparent morphological changes of radish seeds in 1–3 d were observed by adding BPA–LP monomer mixtures and humified precipitates. With the extension of cultivation time, the germination rate and root length of radish seeds increased. Compared with BC, the presence of BPA–LP monomer mixtures (*i.e.*, Hm–P1, Hm–P2, Hm–P3, and Hm–P4) inhibited the seed germination and root length, and the inhibition effect became more obvious with the increase of concentration (Figs. S6 and S7). Notably, certain BPA–LP humified precipitates played a constructive role in seed germination and root length. For instance, compared to BC (3.34 cm), the root length of radish seedlings was reduced to 1.11, 2.01, 2.44, and 2.16 cm by adding 50 mg/L Hm–P1, Hm–P2, Hm–P3, and Hm–P4, respectively, while the root length increased to 4.06, 3.78, 4.40, and 4.03 cm in the presence of La–P1, La–P2, La–P3, and La–P4, respectively. These results suggested that the phytotoxicity of BPA–LP monomer mixtures could be completely removed by generating complex humified products.

To further assess the phytotoxicity of the tested samples, the GI values were also calculated (Table 1). For example, the GI values were 28.82%, 47.31%, 49.68%, and 45.75% by adding Hm–P1, Hm–P2, Hm–P3, and Hm–P4 at 50 mg/L, respectively, implying that BPA-LP monomer mixtures had strong phytotoxicity on radish seeds (GI < 60%). In particular, the GI values increased to 114.29%, 100.43%, 124.05%, and 113.54% (>100%) in the presence of La–P1, La–P2, La–P3, and La–P4, respectively, suggesting that ESH could fully eliminate the phytotoxicity of phenolic compounds by the formation of BPA–LP humified precipitates. These results indicated that certain humified precipitates from ESH had
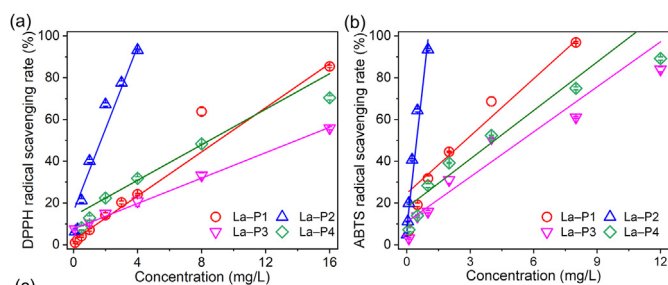
Fig. 4. Linear relationships ($R^2 > 0.95$) obtained for different concentrations of four humified precipitates applied against DPPH/ABTS radicals. DPPH, 2,2-diphenyl-1-picrylhydrazyl; ABTS, 2,2'-azino-bis3-ethylbenzothiazoline-6-sulphonic acid.

Table 1
Seed GI values in phytotoxicity tests of four humified precipitates (*i.e.*, La–P1, La–P2, La–P3 and La–P4) produced from ESH.

Different treatments	GI (%)		
	50 mg/L	100 mg/L	200 mg/L
BC	100	100	100
Hm–P1	28.82	16.06	5.98
La–P1	114.29	105.19	101.81
Hm–P2	47.31	31.81	21.57
La–P2	100.43	121.99	111.66
Hm–P3	49.68	25.73	9.46
La–P3	124.05	127.21	132.73
Hm–P4	45.75	25.77	18.02
La–P4	113.54	112.60	112.45

BC, blank control; GI, germination index; Hm–P1, BPA–Cat–Vaa; Hm–P2, BPA–Cat–Gaa; Hm–P3, BPA–Cat–Fea; Hm–P4, BPA–Cat–Vaa–Gaa–Fea.
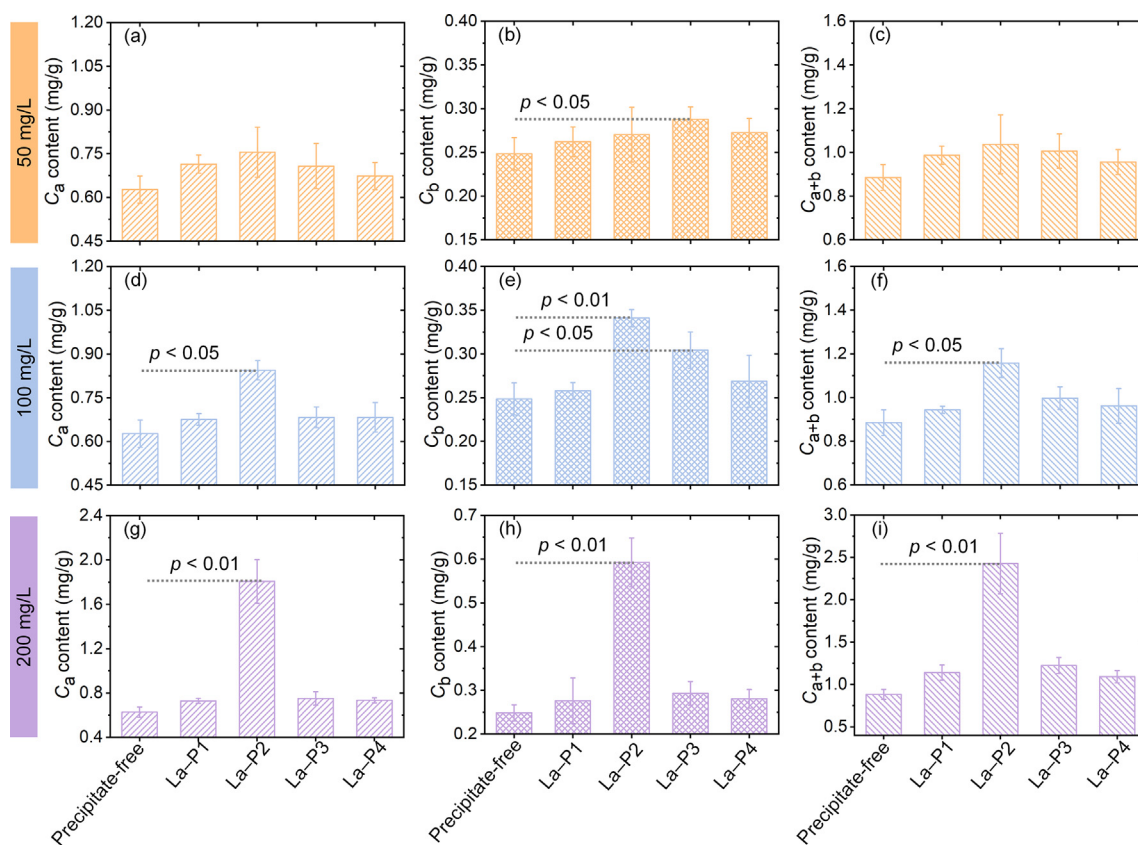
Fig. 5. Effect of four humified precipitates (*i.e.*, La–P1, La–P2, La–P3, and La–P4) on radish seedling chlorophyll a (C_a), chlorophyll b (C_b), and chlorophyll a + b ($C_{a\,+\,b}$) contents in the presence of 250 mM NaCl.

botanical properties similar to auxin, which could accelerate seed germination and root elongation.

3.7. Humified precipitates stimulate radish growth

Biomass is another key index in evaluating plant growth and predicting crop yield. As displayed in Fig. S8, the fresh weights of the shoot and root in BC were 78.72 and 9.40 mg/plant, respectively. The presence of BPA–LP monomer mixtures effectively reduced the biomass of radish seedlings. For example, the fresh weights of shoot and root were 34.37 (4.47), 40.29 (5.18), 35.29 (4.55), and 43.35 (5.93) mg/plant by adding 100 mg/L Hm–P1, Hm–P2, Hm–P3, and Hm–P4, respectively, which were lower than that of BC. The inhibition effect was enhanced with the increase in concentration. It is noted that the total fresh weights of shoot and root were 88.16, 111.63, 97.81, and 96.62 mg/plant in the presence of 100 mg/L La–P1, La–P2, La–P3, and La–P4, respectively, revealing that La–P2 had the highest growth-promoting effect on the biomass of radish seedling. Thus, certain humified precipitates from ESH could stimulate the growth and development of radish seedlings.

Given the above-mentioned results, it is hypothesized that ESH might be a direct and effective strategy to eliminate phenolic contamination and sequester organic carbon by producing functional polymers. Based on the existing literature, the plant growth-promoting mechanisms of humified precipitates were recapitulated in Fig. S9, including three aspects: (1) the humified precipitates contained substrates with a similar structure to auxin, such as indole-3-acetic acid, gibberellic acid, and abscisic acid [7,53]; (2) the humified precipitates interacted with the cell membrane of the root surface and thus triggered a series of biochemical reactions [54,55]; (3) the interaction between humified precipitates and root exudates on the root surface, led to the decomposition of macro-molecular products and the release of plant regulators in root exudates [8,20,56].

3.8. NaCl-tolerance of radish seedlings regulated by humified precipitates

Salinity is one of the dominant abiotic stresses enchaining the use of soil for agriculture due to it hindering the growth and development of plants by NaCl accumulation and water deprivation [57]. As demonstrated in Fig. 5, the humified precipitates increased the chlorophyll content of radish seedlings in the presence of NaCl, compared to the precipitate-free one. Furthermore, as the concentration of humified precipitates increased from 50 to 200 mg/L, the difference in chlorophyll content became more significant. For example, the contents of chlorophyll a, b, and a + b were 1.81, 0.59, and 2.43 mg/g by adding 200 mg/L La–P2, respectively, which were significantly higher than that of the precipitate-free one ($p < 0.01$). It is probably because the humified precipitates alleviated NaCl-triggered osmotic stress and enhanced the activities of nutrient-associated metabolic enzymes, thus making water uptake and nutrient metabolism easier in the root cells [58]. These results disclosed that the formed four precipitates in ESH would contribute to improving plant salt tolerance and agricultural productivity, especially La–P2.

4. Conclusions

This study highlighted the removal and humification of BPA in the presence of LPs by ESH. BPA removal obeyed the pseudo-first-order kinetics. Notably, the presence of LPs significantly promoted BPA conversion during ESH, and the conversion efficiency of BPA was up to 100% within 72 h. Lots of BPA–LP humified products were generated by radical-induced C–C and/or C–O polymerization. The hydrophobic interactions increased in strength with increasing humification time, and thus these humified products could be precipitated from ESH. The formed humification precipitates not only presented obvious aromatic and acidic characteristics, but also had environmental stability and antioxidant capacity. More importantly, they could act as auxin analogs

to promote the growth and development of radish seedlings. Overall, our findings were useful for optimizing practical applications that involved exolaccase-induced decontamination of phenolic contaminants and sequestration of organic carbon. Future research should focus on optimizing the concentration ratios of BPA and LPs to produce high-performance functional polymers.

Author contributions

S.Y.L.: writing-original draft, supervision, funding acquisition, writing-review & editing. D.H.: investigation. K.S.: conceptualization, methodology, formal analysis, investigation, writing-original draft, supervision, funding acquisition, writing-review & editing.

Declaration of competing interests

The authors declare no competing interest.

Acknowledgments

Appendix A. Supplementary data

Supplementary data to this article can be found online at https://doi.org/10.1016/j.eehl.2023.08.006.

References

[1] J. Lehmann, M. Kleber, The contentious nature of soil organic matter, Nature 528 (7580) (2015) 60–68.
[2] S. Wang, Y. Wang, X. He, Q. Lu, Degradation or humification: rethinking strategies to attenuate organic pollutants, Trends Biotechnol. 40 (9) (2022) 1061–1072.
[3] E.P. Reddy, L. Davydov, P. Smirniotis, TiO₂-loaded zeolites and mesoporous materials in the sonophotocatalytic decomposition of aqueous organic pollutants: the role of the support, Appl. Catal. B Environ. 42 (1) (2003) 1–11.
[4] H. Herath, M. Camps-Arbestain, M.J. Hedley, M.U.F. Kirschbaum, T. Wang, R. van Hale, Experimental evidence for sequestering C with biochar by avoidance of CO₂ emissions from original feedstock and protection of native soil organic matter, Gcb Bioenergy 7 (3) (2015) 512–526.
[5] L.M. Colosi, D.J. Burlingame, Q. Huang, W.J.J. Weber, Peroxidase-mediated removal of a polychlorinated biphenyl using natural organic matter as the sole cosubstrate, Environ. Sci. Technol. 41 (3) (2007) 891–896.
[6] J. Yu, H. Xu, D. Wang, H. Sun, R. Jiao, Y. Liu, et al., Variations in NOM during floc aging: effect of typical Al-based coagulants and different particle sizes, Water Res. 218 (2022) 118486.
[7] S. Wei, Z. Li, Y. Sun, J. Zhang, Y. Ge, Z. Li, A comprehensive review on biomass humification: recent advances in pathways, challenges, new applications, and perspectives, Renew. Sustain. Energy Rev. 170 (2022) 112984.
[8] H. Chu, S. Li, K. Sun, Y. Si, Y. Gao, Exolaccase-boosted humification for agricultural applications, iScience 25 (9) (2022) 104885.
[9] R. Guo, Y. Wang, J. Li, X. Cheng, D.D. Dionysiou, Sulfamethoxazole degradation by visible light assisted peroxymonosulfate process based on nanohybrid manganese dioxide incorporating ferric oxide, Appl. Catal. B Environ. 278 (2020) 119297.
[10] S. Li, Y. Sheng, S. Xiao, Q. Liu, K. Sun, Exolaccase propels humification to decontaminate bisphenol A and create humic-like biostimulants, J. Agric. Food Chem. 71 (30) (2023) 11386–11395.
[11] K. Sun, H. Chen, Q. Zhang, S. Li, Q. Liu, Y. Si, Influence of humic acids on fungal laccase-initiated 17α-ethynylestradiol oligomerization: transformation kinetics and products distribution, Chemosphere 258 (2020) 127371.
[12] K. Sun, Q. Liu, S. Li, Y. Qi, Y. Si, MnO₂ nanozyme-driven polymerization and decomposition mechanisms of 17β-estradiol: influence of humic acid, J. Hazard. Mater. 393 (2020) 122393.
[13] J.M. Zou, J.Z. Huang, D.B. Yue, H.C. Zhang, Roles of oxygen and Mn (IV) oxide in abiotic formation of humic substances by oxidative polymerization of polyphenol and amino acid, Chem. Eng. J. 393 (2020) 124734.
[14] G. Hua, J. Kim, D.A. Reckhow, Disinfection byproduct formation from lignin precursors, Water Res. 63 (2014) 285–295.
[15] R.K. Zhang, Y.S. Tan, Y.Z. Cui, X. Xin, Z.H. Liu, B.Z. Li, et al., Lignin valorization for protocatechuic acid production in engineered *Saccharomyces cerevisiae*, Green Chem. 23 (17) (2021) 6515–6526.
[16] M. Hafez, M. Rashad, A.I. Popov, The biological correction of agro-photosynthesis of soil plant productivity, J. Plant Nutr. 43 (19) (2020) 2929–2980.
[17] S. Li, D. Hong, W. Chen, J. Wang, K. Sun, Extracellular laccase-activated humification of phenolic pollutants and its application in plant growth, Sci. Total Environ. 802 (2022) 150005.
[18] Y.C. Zhi, X.N. Li, F. Lian, C.X. Wang, J.C. White, Z.Y. Wang, et al., Nanoscale iron trioxide catalyzes the synthesis of auxins analogs in artificial humic acids to enhance rice growth, Sci. Total Environ. 848 (2022) 157536.
[19] V.K.H. Bui, H.B. Truong, S. Hong, X. Li, J. Hur, Biotic and abiotic catalysts for enhanced humification in composting: a comprehensive review, J. Clean. Prod. 402 (2023) 136832.
[20] S. Li, K. Sun, A. Latif, Y. Si, Y. Gao, Q. Huang, Insights into the applications of extracellular laccase-aided humification in livestock manure composting, Environ. Sci. Technol. 56 (12) (2022) 7412–7425.
[21] Y.C. Zhang, D.B. Yue, X. Wang, W.F. Song, Mechanism of oxidation and catalysis of organic matter abiotic humification in the presence of MnO₂, J. Environ. Sci. 77 (2019) 167–173.
[22] X. Zhang, Y. Zong, L. Xu, Y. Mao, D. Wu, Enhanced abiotic integrated polyphenol-Maillard humification by Mg/Fe layered double hydroxide (LDH): role of Fe (III)-polyphenol complexation, Chem. Eng. J. 425 (2021) 130521.
[23] M. Hong, J. Chen, E.Y.X. Chen, Polymerization of polar monomers mediated by main-group Lewis acid-base pairs, Chem. Rev. 118 (20) (2018) 10551–10616.
[24] R. Nishimoto, S. Fukuchi, G. Qi, M. Fukushima, T. Sato, Effects of surface Fe (III) oxides in a steel slag on the formation of humic-like dark-colored polymers by the polycondensation of humic precursors, Colloids Surf. A Physicochem. Eng. Asp. 418 (2013) 117–123.
[25] K. Sun, S. Li, Y. Si, Q. Huang, Advances in laccase-triggered anabolism for biotechnology applications, Crit. Rev. Biotechnol. 41 (7) (2021) 969–993.
[26] M. Mogharabi, M.A. Faramarzi, Laccase and laccase-mediated systems in the synthesis of organic compounds, Adv. Synth. Catal. 356 (5) (2014) 897–927.
[27] N.M. Mahmoodi, M.H. Saffar-Dastgerdi, Clean laccase immobilized nanobiocatalysts (graphene oxide-zeolite nanocomposites): from production to detailed biocatalytic degradation of organic pollutant, Appl. Catal. B Environ. 268 (2020) 118443.
[28] C.L. Zhuo, X. Wang, M. Docampo-Palacios, B.C. Sanders, N.L. Engle, T.J. Tschaplinski, et al., Developmental changes in lignin composition are driven by both monolignol supply and laccase specificity, Sci. Adv. 8 (10) (2022) eabm8145.
[29] K. Sun, X. Cheng, J. Yu, L. Chen, J. Wei, W. Chen, et al., Isolation of *Trametes hirsuta* La-7 with high laccase-productivity and its application in metabolism of 17β-estradiol, Environ. Pollut. 263 (2020) 114381.
[30] O.E. Adelakun, T. Kudanga, I.R. Green, M. le Roes-Hill, S.G. Burton, Enzymatic modification of 2,6-dimethoxyphenol for the synthesis of dimers with high antioxidant capacity, Process Biochem. 47 (12) (2012) 1926–1932.
[31] M.R. Prusty, S.R. Kim, R. Vinarao, F. Entila, J. Egdane, M.G.Q. Diaz, et al., Newly identified wild rice accessions conferring high salt tolerance might use a tissue tolerance mechanism in leaf, Front. Plant Sci. 9 (2018) 417.
[32] Y.H. Chuang, D.L. McCurry, H. Tung, W.A. Mitch, Formation pathways and trade-offs between haloacetamides and haloacetaldehydes during combined chlorination and chloramination of lignin phenols and natural waters, Environ. Sci. Technol. 49 (24) (2015) 14432–14440.
[33] J. Sternberg, O. Sequerth, S. Pilla, Green chemistry design in polymers derived from lignin: review and perspective, Prog. Polym. Sci. 113 (2021) 101344.
[34] H. Catherine, M. Penninckx, D. Frédéric, Product formation from phenolic compounds removal by laccases: a review, Environ. Technol. Innov. 5 (2016) 250–266.
[35] S.A. Onaizi, M. Alshabib, The degradation of bisphenol A by laccase: effect of biosurfactant addition on the reaction kinetics under various conditions, Sep. Purif. Technol. 257 (2021) 117785.
[36] K. Sun, Q. Liu, J. Liu, S. Li, X. Qi, M. Chen, et al., New insights into humic acid-boosted conversion of bisphenol A by laccase-activated co-polyreaction: kinetics, products, and phytotoxicity, J. Hazard. Mater. 436 (2022) 129269.
[37] M. Arefmanesh, T.V. Vuong, S. Nikafshar, M. Wallmo, M. Nejad, E.R. Master, Enzymatic synthesis of kraft lignin-acrylate copolymers using an alkaline tolerant laccase, Appl. Microbiol. Biotechnol. 106 (8) (2022) 2969–2979.
[38] K.H. Nguyen, V.D. Dao, T.T.H. Ngo, T.H.T. Nguyen, Q.T. Nguyen, T.T. Le, Removal of bisphenol A using laccase-catalyzed electrooxidation in the presence of humic acid, CLEAN Soil Air Water 50 (9) (2022) 2100368.
[39] F.J. Rodríguez, P. Schlenger, M. García-Valverde, Monitoring changes in the structure and properties of humic substances following ozonation using UV-Vis, FTIR and ¹H NMR techniques, Sci. Total Environ. 541 (2016) 623–637.
[40] A.M. Tadini, I.C. Constantino, A. Nuzzo, R. Spaccini, A. Piccolo, A.B. Moreira, et al., Characterization of typical aquatic humic substances in areas of sugarcane cultivation in Brazil using tetramethylammonium hydroxide thermochemolysis, Sci. Total Environ. 518 (2015) 201–208.
[41] T. Grinhut, N. Hertkorn, P. Schmitt-Kopplin, Y. Hadar, Y. Chen, Mechanisms of humic acids degradation by white rot fungi explored using ¹H NMR spectroscopy and FTICR mass spectrometry, Environ. Sci. Technol. 45 (7) (2011) 2748–2754.
[42] J. Rosselgong, S.P. Armes, Quantification of intramolecular cyclization in branched copolymers by ¹H NMR spectroscopy, Macromolecules 45 (6) (2012) 2731–2737.
[43] N. Aktaş, A. Tanyolaç, Reaction conditions for laccase catalyzed polymerization of catechol, Bioresour. Technol. 87 (3) (2003) 209–214.
[44] S. Camarero, A.I. Cañas, P. Nousiainen, E. Record, A. Lomascolo, M.J. Martínez, et al., *p*-Hydroxycinnamic acids as natural mediators for laccase oxidation of recalcitrant compounds, Environ. Sci. Technol. 42 (17) (2008) 6703–6709.

[45] J.R. Jeon, P. Baldrian, K. Murugesan, Y.S. Chang, Laccase-catalysed oxidations of naturally occurring phenols: from *in vivo* biosynthetic pathways to green synthetic applications, Microb. Biotechnol. 5 (3) (2012) 318–332.

[46] J. Liu, H. Liu, L. Chen, Y. An, X. Jin, X. Li, et al., Study on the removal of lignin from pre-hydrolysis liquor by laccase-induced polymerization and the conversion of xylose to furfural, Green Chem. 24 (4) (2022) 1603–1614.

[47] M.B. Agustin, D.M. de Carvalho, M.H. Lahtinen, K. Hilden, T. Lundell, K.S. Mikkonen, Laccase as a tool in building advanced lignin-based materials, ChemSusChem 14 (21) (2021) 4615–4635.

[48] C. Zhong, H. Zhao, H. Cao, Q. Huang, Polymerization of micropollutants in natural aquatic environments: a review, Sci. Total Environ. 693 (2019) 133751.

[49] S. Ganda, M.H. Stenzel, Concepts, fabrication methods and applications of living crystallization-driven self-assembly of block copolymers, Prog. Polym. Sci. 101 (2020) 101195.

[50] M. Matsumoto, L. Sutrisno, K. Ariga, Covalent nanoarchitectonics: polymer synthesis with designer structures and sequences, J. Polym. Sci. 61 (10) (2023) 861–869.

[51] J. Rumpf, R. Burger, M. Schulze, Statistical evaluation of DPPH, ABTS, FRAP, and Folin-Ciocalteu assays to assess the antioxidant capacity of lignins, Int. J. Biol. Macromol. 233 (2023) 123470.

[52] R. Wołosiak, B. Drużyńska, D. Derewiaka, M. Piecyk, E. Majewska, M. Ciecierska, et al., Verification of the conditions for determination of antioxidant activity by ABTS and DPPH assays-A practical approach, Molecules 27 (1) (2022) 50.

[53] F. Yang, C. Tang, M. Antonietti, Natural and artificial humic substances to manage minerals, ions, water, and soil microorganisms, Chem. Soc. Rev. 50 (10) (2021) 6221–6239.

[54] T.C. de Aguiar, D.F. de Oliveira Torchia, T.A.T. de Castro, O.C.H. Tavares, S. de Abreu Lopes, L. de Souza da Silva, et al., Spectroscopic-chemometric modeling of 80 humic acids confirms the structural pattern identity of humified organic matter despite different formation environments, Sci. Total Environ. 833 (2022) 155133.

[55] S. Nardi, M. Schiavon, O. Francioso, Chemical structure and biological activity of humic substances define their role as plant growth promoters, Molecules 26 (8) (2021) 2256.

[56] I. Basile-Doelsch, J. Balesdent, S. Pellerin, Reviews and syntheses: the mechanisms underlying carbon storage in soil, Biogeosciences 17 (21) (2020) 5223–5242.

[57] N. Hmaeid, M. Wali, O.M.B. Mahmoud, J.J. Pueyo, T. Ghnaya, C. Abdelly, Efficient rhizobacteria promote growth and alleviate NaCl-induced stress in the plant species *Sulla carnosa*, Appl. Soil Ecol. 133 (2019) 104–113.

[58] A. El Moukhtari, C. Cabassa-Hourton, M. Farissi, A. Savouré, How does proline treatment promote salt stress tolerance during crop plant development? Front. Plant Sci. 11 (2020) 1127.